Check for updates

ORIGINAL PAPER

physica status solidi a
www.pss-a.com

Optimizing the Stoichiometry of Ga_2O_3 Grown by RF-Magnetron Sputter Deposition by Correlating Optical Properties and Growth Parameters

Philipp Schurig, Marcel Couturier, Martin Becker, Angelika Polity, and Peter Jens Klar*

β-Ga_2O_3 thin films are deposited by radiofrequency (RF)-magnetron sputtering on quartz and c-sapphire substrates using a ceramic stoichiometric Ga_2O_3 target and a constant flux of argon process gas. Oxygen flux, heater power, and sputtering power are varied in the synthesis of the layers. The resulting Ga_2O_3 layers are analyzed in terms of their structural and optical properties. Based on this analysis, the process parameters leading to the formation of an optimized β-Ga_2O_3 layer are identified. The main challenge in obtaining the stoichiometric β-Ga_2O_3 thin films by sputter deposition is to overcome the influence of a strong preferential sputtering of Ga from the ceramic target. This can be achieved by adding a suitable fraction of oxygen to the argon process gas used in the deposition process. Furthermore, it is demonstrated that the refractive index dispersion of β-Ga_2O_3 depends strongly on its composition. Thus, a combined analysis of refractive index dispersion and optical bandgap position may serve as a valuable preliminary probe of the thin film's composition.

1. Introduction

The generation of energy from renewable energy sources, for example, conversion of solar energy into electric energy by solar cells, is still a major research area. The driving force is to reduce fossil fuel consumption and, thus, to stop, or at least postpone, global warming. It requires a mass production of solar cells as well as an efficient use of all available areas for installing such devices for photovoltaics to yield a viable contribution to the world's energy supply.

Transparent conducting oxides (TCOs), which exhibit almost metal-like conductivities in addition to a large bandgap (>3 eV), play an important role in thin-film photovoltaics concepts.[1,2] These serve as transparent top contacts forming the p–n junction to a smaller bandgap absorber in thin-film photovoltaics. The quest for absorber materials based on abundant chemical elements is on and necessary to realize corresponding thin-film solar cells on mass production levels. Thin-film photovoltaics on glass substrates and based on abundant semiconductor materials may offer a cheap alternative to the established technologies. Another interesting possibility for further integration of photovoltaics into modern life is to develop transparent solar cells, for example, windows that may also act as solar cells and contribute to the energy supply.[3] As this approach requires materials that are conductive and transparent at the same time, TCOs are likely candidate materials for this purpose.[4]

The p–n junction is the central building block of a thin-film photovoltaic cell as it generates the built-in electric field to separate charge carriers generated by absorption of light. Recently, cuprous oxide, Cu_2O, with its bandgap of 2.1 eV is discussed as a suitable and promising p-type absorber material[5–7] based on abundant chemical elements. To tap the full potential of Cu_2O as absorber material in thin-film solar cells, it needs to be combined with a suitable n-type semiconductor. "Suitable" means that the band alignment at the junction does not exhibit high-band offsets, in particular, in the conduction band. β-Ga_2O_3 is discussed as a promising candidate, because of its low-electron affinity close to that of Cu_2O, it exhibits a very low discontinuity in the conduction band.[8,9] Furthermore, Ga_2O_3 has a large bandgap close to 5 eV[10–12] and thus forms an ideal top contact on Cu_2O, when doped n-type. In case of a transparent solar cell, both constituents on either side of the junction, p- and n-type semiconductors, have to be transparent. Nowadays n-type semiconducting transparent materials are state of the art, but suitable p-type conductors still need to be identified.

For the reasons outlined earlier, there is a considerable interest in Ga_2O_3 in the context of photovoltaics. The material and its processing offer various degrees of freedom for optimizing its structure for a specific application. Five different crystalline phases of Ga_2O_3, denoted as α, β, γ, δ, and ε phase, are known to date.[13] The β-phase has the highest thermal and chemical

P. Schurig, M. Couturier, Dr. M. Becker, Dr. A. Polity, Prof. P. J. Klar
Institute for Experimental Physics I and Center for Materials Research (LaMa)
Justus Liebig University Giessen
Giessen, Germany
E-mail: martin.becker@exp1.physik.uni-giessen.de

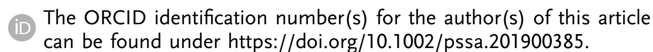
The ORCID identification number(s) for the author(s) of this article can be found under https://doi.org/10.1002/pssa.201900385.

© 2019 The Authors. physica status solidi (a) applications and materials science published by Wiley-VCH GmbH. This is an open access article under the terms of the Creative Commons Attribution-NonCommercial-NoDerivs License, which permits use and distribution in any medium, provided the original work is properly cited, the use is non-commercial and no modifications or adaptations are made.

The copyright line for this article was changed on 4 February 2021 after original online publication.

DOI: 10.1002/pssa.201900385

stability among those five phases.[14,15] Moreover, the crystal structure, conductivity, as well as optical bandgap of Ga_2O_3 can be influenced by the changes in process parameters or by post-thermal treatment.[16,17] Thus, a controlled manufacturing process for β-Ga_2O_3 is a hot topic of applied research in photovoltaics.

Ga_2O_3 thin films may be prepared by various methods, including molecular beam epitaxy (MBE),[18–20] metal-organic chemical vapor deposition (MOCVD),[21] pulsed laser deposition (PLD),[11,22] sol gel,[23,24] chemical vapor deposition (CVD),[25–27] and sputtering techniques.[15,17,28–31] The reported growth rates of stoichiometric Ga_2O_3 thin films are comparatively low. Typical growth rates of Ga_2O_3 thin films grown by MBE and PLD are 0.04[20] to 0.09[32] and 0.22 $\mu m\,h^{-1}$,[33] respectively. An increase in the growth rate of Ga_2O_3 films is desirable in terms of mass production of devices and can be obtained by means of RF-magnetron sputtering with deposition rates $>1\ \mu m\,h^{-1}$.[17]

In this study, we discuss the deposition of Ga_2O_3 thin films on quartz and c-sapphire substrates using RF-magnetron sputtering. Heating power, sputtering power, as well as oxygen flow were varied. Subsequently, β-Ga_2O_3 films were investigated to optimize the deposition conditions according to β-Ga_2O_3 growth. Refractive index dispersion was determined for stoichiometric and nonstoichiometric Ga_2O_3 thin films and compared with the limited data in literature available on sputtered Ga_2O_3 samples.[30,34]

2. Experimental Section

We deposited Ga_2O_3 thin films on quartz and c-sapphire substrates by RF-magnetron sputtering. In sputtering, ions of the process gas—in our case, a gas mixture of inert Ar and reactive O_2—impinge onto a target, here a Ga_2O_3 ceramic target and sputter off target atoms. The target atoms react with the reactive species of the process gas and form a film, here a Ga_2O_3 film, on the substrate, which is located opposite the target surface. Prior to each deposition, the substrates were cleaned with acetone and methanol in an ultrasonic bath for 3–5 min and then dried with nitrogen. Subsequently, the substrates were mounted in a cylindrical sputter chamber (base pressure of 5×10^{-7} mbar) at a distance of 5 cm below the target to assure lateral homogeneity.

Here, we discuss three series of samples. Throughout each series a specific process parameter was varied systematically, while all the other process parameters were kept constant (**Table 1**). The variables chosen were Ar:O_2 ratio in series I, substrate temperature in series II, and RF power in series III. In case of series II, the substrate temperature was varied by adjusting the heating power of the temperature controller (model Eurotherm 2408). The interval of 465–1440 W nonlinearly translates to a temperature window between 385 and 581 °C on the substrate surface in vacuum, without a plasma being present. A distinct characteristic is given by an interplay of the substrate's thermal conductivity and its effectiveness in emitting energy as thermal radiation. The actual growth temperatures (surface temperatures) may be considerably higher depending on the RF power coupled into the plasma of the process gas and the distinct thermal directional characteristic. This enhancement of the surface temperature by the presence of the plasma is estimated to be up to 200 °C at the highest RF power used. The RF power was generated by a Dressler CESAR 1312 system equipped with a Dressler VM 1500 AW matching network and was varied between 50 and 200 W. It should be noted that the surface temperatures in vacuum for quartz substrates are 50 °C lower than those for sapphire substrates at the highest heating power. This finding is related to the lower thermal conductivity of quartz in the temperature range relevant in the growth process.

The films were analyzed by X-ray diffraction (XRD, Siemens D 5000) in a Θ–2Θ geometry. Optical transmittance at normal incidence ($\beta = 0°$) and relative specular reflectance close to normal incidence ($\beta = 6°$) were recorded using a PerkinElmer Lambda 900 spectrometer. The influence of the substrate was eliminated by measuring the substrate baseline prior to thin film deposition. Most thin films discussed possess layer a thicknesses $>1\ \mu m$.

Table 1. Parameters used in sputter processes for depositing sample series I–III.

Series	Ar flux [sccm]	O_2 flux [sccm]	RF power [W]	Heating power [W]
I	45	8–15	200	465
II	45	12.5	200	465–1440
III	45	12.5	50–200	1135

3. Results and Discussion

Figure 1a–c illustrates the X-ray diffractograms of Ga_2O_3 layers of series I, II, and III grown on quartz substrates. The findings are very similar in case of the series on sapphire substrates, but the corresponding XRD traces are dominated by strong and sharp sapphire reflections and are, thus, not shown here.

In series I, no significant change arises as a function of oxygen flux, that is, variation of the Ar:O_2 fraction of the process gas used in deposition (Figure 1a). However, this is somewhat expected because when using a stoichiometric target, a slight variation of the O:Ga ratio in gallium sesquioxide seems more likely than the formation of suboxide phases. Heating power was at the lowest setting of 465 W, and RF power coupled into the process plasma was 200 W. All diffractograms reveal rather broad signals at about 30°, 35°, 45°, 57°, and 64°. Characteristic reflections of β-Ga_2O_3 are given on top of the figure and are indicated by green vertical lines. A comparison with reflections reveals the polycrystalline character of deposited layers. This is in contrast to the findings of Kang, who found Bragg reflections only for the {–201} β-Ga_2O_3 family of planes on c-sapphire substrates and concluded that this is the preferred orientation in surface-normal direction.[29] It should be noted that in the findings of Kang thin films were deposited at 645 °C, whereas our samples (Figure 1a) were grown at temperatures <600 °C. Thus, we believe a minimum growth temperature, among others, is a mandatory condition for obtaining β-Ga_2O_3 thin films on c-sapphire substrates with a preferential orientation. A similar behavior was found for β-Ga_2O_3 sputter grown on silicon substrates where the as-deposited samples exhibited an amorphous XRD pattern, and annealing temperatures ≥900 °C were necessary for obtaining polycrystalline material.[15,17]

© 2019 The Authors. physica status solidi (a) applications and materials science published by Wiley-VCH GmbH

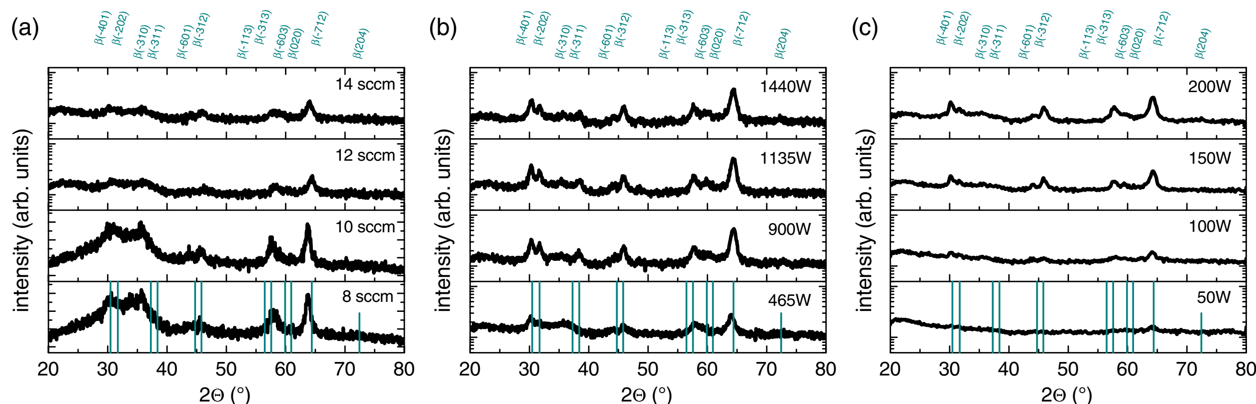

Figure 1. a) X-ray diffractograms of Ga_2O_3 grown on quartz. Changing the Ar:O_2ratio in sputter atmosphere does not alter crystallinity significantly, whereas several orientations are observed. This polycrystallinity is also verified for b) series II (substrate temperature) and c) series III (RF power).

Figure 1b shows the results of series II where heater power and, thus, surface temperatures of the substrate were varied. Ar and O_2 flux were set to 45 and 12.5 sccm, respectively, and the RF power coupled into the process plasma was again 200 W. Crystallinity improved on increasing the heater power from 465 to 900 W, indicated by the sharpening of the reflections. However, no further improvement was observable >900 W. A heating power of 1135 W; and Ar and O_2 flux set to 45 and 12.5 sccm, respectively, were kept constant in series III, whereas the RF power and consequently also the kinetic energy of the ion species of the process gas were varied between 50 and 200 W. The diffractograms of the corresponding samples (Figure 1c) show first a slight increase in intensity and number of peaks toward a higher RF power up to 150 W. A further increase in the RF power to 200 W resulted in no additional improvement of crystallinity. However, increasing the RF power is accompanied with a significant gain in the growth rate.[35,36] Thus, we believe that increasing the layer thickness by increasing the RF power while maintaining the deposition temperature counteracts a possible improvement in crystallinity due to more disordered growth.

Figure 2a depicts the optical transmittance spectra of Ga_2O_3 layers of series I on quartz and c-sapphire substrates in the wavelength range of 260–400 nm. Above a wavelength of 360 nm, transmittance of all thin films was about 80–100%, presenting interference oscillations between light transmitted directly and light reflected at the back and front interfaces prior to being transmitted. Using the dispersion relation of refractive index given by Rebien et al. for RF-magnetron-sputtered samples,[34] whose composition was monitored by Rutherford backscattering, layer thickness d may be derived from the interference pattern. The corresponding values are shown in Figure 2c together with thickness values deduced from scanning electron microscopy (SEM) images of the edge of cleaved samples. The comparison indicates that—as expected from the variation of growth parameters, in particular, oxygen flux—the assumption of a stoichiometric sample is not valid in all cases. Indeed, preliminary measurements by X-ray photoelectron spectroscopy (XPS) show that samples of the oxygen flux series deviated from O:Ga = 1.5. We evaluated core-level O 1s, Ga 2p, and Ga 3d and found Ga concentrations up to 44% for low oxygen flux, whereas values close to 40% were found for highest oxygen fluxes used in series I.

Therefore, we decided to use the values of layer thickness obtained by SEM analysis of cleaved edges in conjunction with

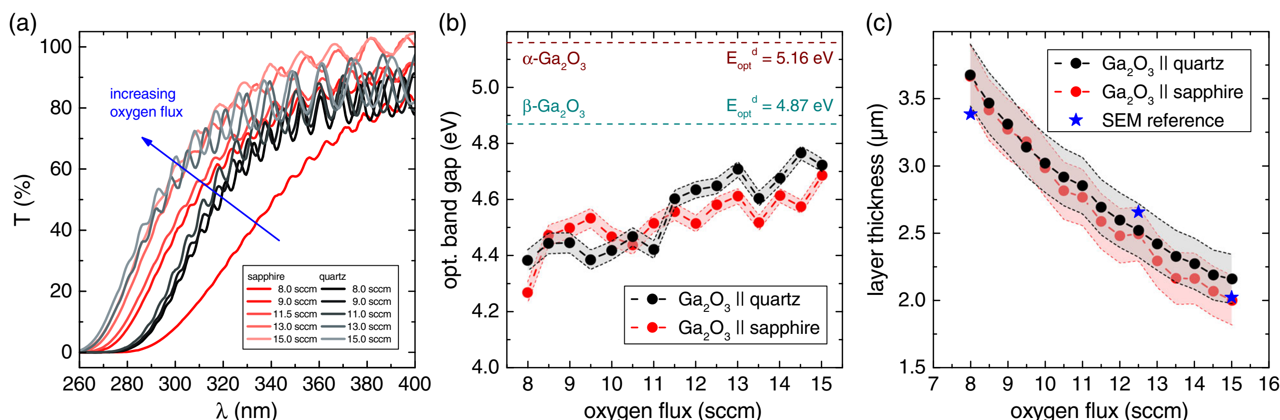

Figure 2. a) Representative optical transmittance spectra of Ga_2O_3 layers, deposited at different oxygen fluxes. Qualitatively, the dependence of b) optical bandgap and c) layer thickness is the same for Ga_2O_3 thin films deposited on quartz and c-plane sapphire, respectively. Asterisks in (c) denote the thicknesses determined by SEM analysis. Error margins given in (b) and (c) arise due to error in the refractive index used.[34]

© 2019 The Authors. physica status solidi (a) applications and materials science published by Wiley-VCH GmbH

interference oscillations observed to derive refractive index dispersions of selected Ga_2O_3 samples grown. This allowed us to assess the magnitude of refractive index variation introduced by nonstoichiometry. Results for selected samples of all three series are shown in **Figure 3**. The corresponding growth parameters are given in the legend of the figure; the error bars represent uncertainties in layer thicknesses and the extremas' wavelengths in optical transmittance spectra. For clarity, only one error bar is shown per sample. The curvature of extracted dispersion relations is comparable with that of dispersion relation derived by Rebien et al.[34] independent of composition. However, the absolute values of nonstoichiometric samples are considerably higher. This can be best seen in the long-wavelength regime where stoichiometric, crystalline β-Ga_2O_3 possesses a refractive index of about 1.9 in accordance with previously reported results,[30,34] and nonstoichiometric materials exhibit values

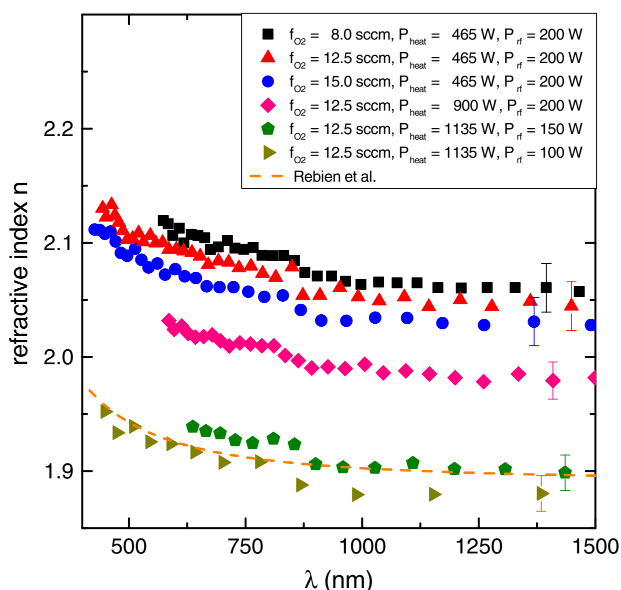

Figure 3. Refractive index dispersion of selected samples highlighting that nonstoichiometry triggers defective evaluation of thickness and optical bandgaps.

almost up to 2.1. The analysis of the growth parameters yields that only the refractive index dispersion of samples prepared at a high heater power (i.e., high surface temperatures) and rather low RF power (i.e., low kinetic energy of ionic species of the plasma) match the dashed line representing the refractive index dispersion of stoichiometric β-Ga_2O_3. The error margins to the data points in **Figure** 2 and 4 represents the uncertainty due to an unknown degree of nonstoichiometry of the samples and corresponding uncertainties in the layer thicknesses. This uncertainty will not alter the trends and interpretations given in what follows. Furthermore, these findings will be important for future investigations of nonstoichiometric β-Ga_2O_3 or even Ga_2O_3-based alloys.

In the spectral range >400 nm, reflectance and transmission approximately add up to 100%, whereas <360 nm, measured transmittance drops due to absorption in the thin β-Ga_2O_3 films. At wavelengths λ where absorption dominates, the absorption coefficient α may be extracted using:

$$T(\lambda) = [1 - R(\lambda)] \cdot \exp(-\alpha(\lambda)d) \quad (1)$$

where α denotes the absorption coefficient, d the layer thickness, T the transmittance, and R the reflectance. The optical bandgap of Ga_2O_3 film can be estimated using Tauc's approach,[37] assuming a direct transition at the bandgap. Plotting α^2 versus $\hbar\omega$; and extrapolating the linear part of the curve to the abscissa yields the energy of the optical bandgap of the material studied, independent of its layer thickness.

For the samples of series I, on quartz as well as on sapphire, a shift in this onset of optical absorption toward lower wavelengths was found with increasing oxygen flux (Figure 2a). The optical bandgap of β-Ga_2O_3 layers increases with increasing oxygen flux (Figure 2b) and approaches the value reported for the bandgap of stoichiometric β-Ga_2O_3 of 4.87 eV from below. In agreement with the refractive index analysis, this behavior indicates that these samples are not stoichiometric and probably still oxygen-deficient.[14] The bandgap increases as the density of defects induced by oxygen deficiency is reduced with increasing oxygen flux. As the target consists of stoichiometric Ga_2O_3 and additional oxygen was used in the gas mixture, it may be anticipated, at first sight, that excess oxygen is present in the plasma

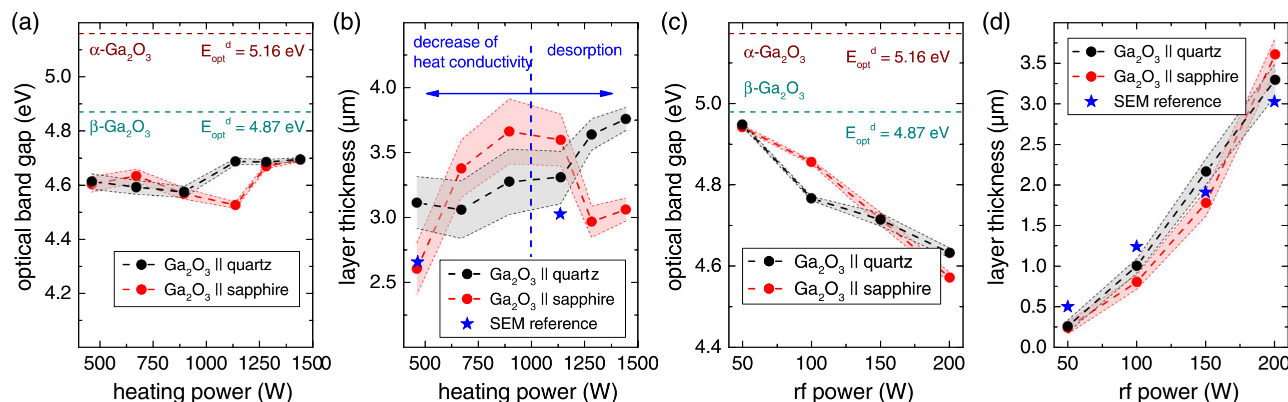

Figure 4. a,c) Optical bandgaps and b,d) layer thicknesses as a function of a,b) heater power applied during growth as well as c,d) RF power applied during growth. Asterisks in (b) and (d) denote the thicknesses determined by SEM analysis. Error margins given in (a–d) arise due to error in the refractive index used.[34]

© 2019 The Authors. physica status solidi (a) applications and materials science published by Wiley-VCH GmbH

and deposited layer. However, this consideration is in contrast with the optical data. Therefore, we believe that strong preferential sputtering occurs on the target, that is, gallium exhibits a much higher sputter yield than oxygen from Ga_2O_3 surfaces. Furthermore, in the same series of samples, we found that the growth rate was reduced with increasing oxygen flux as reflected by the layer thicknesses plotted versus oxygen flow in Figure 2c. The reason is that, as described earlier, the density of the process gas increased when the oxygen flow increased. As a consequence, the mean free path of the species in the plasma reduced and the rate of collisions of ions (which possess sufficient kinetic energy to sputter atoms off the target) with the target also reduced.[38] Moreover, the likelihood of the formation of negatively charged oxygen species in the plasma increased. Negatively charged ions accelerated toward the sample holder, which act as the anode. These oxygen species may etch the thin-film surface, further reducing the growth rate.[39]

Series II was deposited at different heating powers (Table 1) to see its impact on the thin-film growth. Figure 4b clearly reveals that the amount of heating power also affects the growth rate in addition to the degree of crystallinity. Furthermore, the trends observed for layers on quartz glass and sapphire substrates differ. The growth rate of the former increased steadily, whereas that of the latter exhibited a maximum in the intermediate heater power range. This behavior can be understood as follows. The diffusion rate of gallium and oxygen atoms on the substrate surface increased with increasing substrate temperature. It is the temperature that determines decisively how efficiently the atoms can arrange themselves on the surface. In general, a higher mobility of the species on the surface enables comparatively faster layer growth and higher crystallinity. However, the temperature can also be too high in the sense that the thermal energy is large enough to enable desorption of atomic species from the surface. Here the properties of the substrate come into play as the energy transfer from the heater arrangement to the substrate surface is determined, among others, by the substrate's thermal conductivity. The results in Figure 4b reveal clearly this influence on the substrate as quartz glass possesses lower thermal conductivity compared with sapphire.[40] The surface temperature of sapphire is about 50 °C higher than that of quartz glass at high heater powers. Note that this temperature difference was measured for substrates without plasma impact. Thus, the actual temperature difference might be even higher. In any case, the temperature corresponding to the onset of atomic desorption will be reached at a lower heater power in growth on sapphire surfaces, already at about 1000 W, than in growth on quartz glass, where it probably lies outside the accessible heater power range of the sputter system.

Figure 4a shows the behavior of optical bandgaps of Ga_2O_3 layers grown on the two types of substrates depending on substrate temperature. The bandgaps were again determined following Tauc's approach.[37] The observed trends were very similar, and even at the highest temperatures (heating powers), the value of 4.87 eV reported for the optical gap of stoichiometric bulk β-Ga_2O_3 could not be reached. However, the bandgap values were higher than those found for series I, somewhat indicating that growth at higher temperatures yielded a Ga_2O_3 material of better crystallinity, but probably not stoichiometric yet. For example, Sampath Kumar et al. showed that increasing the substrate temperature led to a reduction of the O:Ga ratio in their deposited Ga_2O_3 layers.[14] At room temperature, they observed an O:Ga ratio of 1.6, whereas at a process temperature of 600 °C, a stoichiometric ratio of about 1.5 was evaluated. Already at 300 °C, a clear trend toward an O:Ga ratio of 1.5 was shown.[14] Ramana et al. observed the same trend in their XPS analysis.[30] Thus, in any case, heating power plays an important role; however, an interplay of various factors such as crystal quality, defect structure, surface morphology, grain size, and composition might also affect the optical properties, rendering exact one-to-one transfer of conclusions difficult.

The results of Ga_2O_3 samples of series III grown at a high substrate temperature with different RF powers coupled to the plasma of the process gas are shown in Figure 4c,d. Clear trends were observed, which were similar for layers on both types of substrates. First, it should be noted (Figure 4c) that the samples of series III grown at the lowest RF power exhibited optical bandgaps closest to the theoretical value of stoichiometric β-Ga_2O_3. With increasing RF power, however, the optical bandgap values of Ga_2O_3 significantly decreased in a linear fashion. The growth rate (Figure 4d) showed the opposite trend and increased linearly with increasing RF power coupled into the plasma of the process gas. The results can be explained as follows. The lower the RF power coupled into the plasma, the less the kinetic energy of the process gas ions impinging on the target. The discussion of series I already showed that preferential sputtering is a major issue when using a Ga_2O_3 ceramic target in the growth process as the sputter yields of Ga and O were very different for this material. At the lowest RF power, the effect of preferential sputtering can be compensated by the excess oxygen in the process gas. Thus, the particle flux toward the substrate corresponds to the right stoichiometry. Furthermore, due to the low sputter rates at 50 W RF power, the atoms deposited on the substrate had more time to reach their positions and to form a film of better crystalline quality. We believe that weak X-ray diffractograms in Figure 1c obtained for the layers of series III grown at low RF power were rather due to small thicknesses of those films than due to lower crystalline quality, although a contribution of enhanced amorphization cannot be ruled out entirely.

4. Conclusions

Ga_2O_3 thin films were deposited by RF-magnetron sputtering from a ceramic Ga_2O_3 target onto quartz and c-sapphire substrates. Oxygen flux, heating power, and RF power coupled into the plasma of the process gas were varied systematically. Stoichiometric β-Ga_2O_3 polycrystalline thin films were obtained at moderate growth temperatures of about 600 °C, when a low RF power was used and the process gas contained excess oxygen. Excess oxygen is required to compensate the excess Ga in the particle flux toward the substrate arising from a strong preferential sputtering of Ga species from the target. The growth rate found for the best β-Ga_2O_3 thin-film material was rather low; however, the layer thickness determined still translates to a growth rate of 0.25 $\mu m\,h^{-1}$, a value comparable to the largest rates given in literature for other growth methods. Moreover, our results suggest that a low growth rate is not an intrinsic problem and may even be enhanced by coupling higher RF power into the plasma and simultaneously increasing the fraction of oxygen

© 2019 The Authors. physica status solidi (a) applications and materials science published by Wiley-VCH GmbH

in the process gas. Refractive index dispersions and optical bandgaps extracted from UV/Vis optical transmittance and reflection spectra were successfully used to identify stoichiometric β-Ga_2O_3. In particular, we demonstrated that the refractive index dispersion of nonstoichiometric β-Ga_2O_3 strongly deviates from that of a stoichiometric material, an aspect that may play a role in optimizing the antireflection behavior of Ga_2O_3 transparent contacts on thin-film solar cells.

Acknowledgements

Financial support was provided by the DFG via the RTG (Research Training Group) 2204, "Substitute Materials for Sustainable Energy Technologies."

Conflict of Interest

The authors declare no conflict of interest.

Keywords

gallium oxide, refractive indexes, RF-magnetron sputter deposition, thin films

Received: May 9, 2019
Revised: July 31, 2019
Published online: August 25, 2019

[1] M. Grundmann, H. Frenzel, A. Lajn, M. Lorenz, F. Schein, H. von Wenckstern, *Phys. Status Solidi A* **2010**, *207*, 1437.
[2] P. D. C. King, T. D. Veal, *J. Phys.: Condens. Matter* **2011**, *23*, 334214.
[3] A. A. Husain, W. Z. Hasan, S. Shafie, M. N. Hamidon, S. S. Pandey, *Renew. Sustain. Energy Rev.* **2018**, *94*, 779.
[4] E. Fortunato, D. Ginley, H. Hosono, D. C. Paine, *MRS Bull.* **2007**, *32.3*, 242.
[5] B. K. Meyer, A. Polity, D. Reppin, M. Becker, P. Hering, P. J. Klar, T. Sander, C. Reindl, J. Benz, M. Eickhoff, C. Heiliger, M. Heinemann, J. Bläsing, A. Krost, S. Shokovets, C. Müller, C. Ronning, *Phys. Status Solidi B* **2012**, *249*, 1487.
[6] B. Kramm, A. Laufer, D. Reppin, A. Kronenberger, P. Hering, A. Polity, B. K. Meyer, *Appl. Phys. Lett.* **2012**, *100*, 094102.
[7] K. P. Hering, R. E. Brandt, B. Kramm, T. Buonassisi, B. K. Meyer, *Energy Proc.* **2014**, *44*, 32.
[8] J. Brehm, *Synthese und Charakterisierung nanokristalliner transparenter Halbleiteroxide*. Cuvillier-Verlag, Göttingen **2005**, p. 3.
[9] T. Minami, Y. Nishi, T. Miyata, *Appl. Phys. Express* **2013**, *6*, 044101.
[10] H. H. Tippins, *Phys. Rev.* **1965**, *140*, A316.
[11] M. Orita, H. Ohta, M. Hirano, H. Hosono, *Appl. Phys. Lett.* **2000**, *77*, 4166.
[12] H. He, R. Orlando, M. A. Blanco, R. Pandey, E. Amzallag, I. Baraille, M. Rérat, *Phys. Rev. B* **2006**, *74*, 195123.
[13] H. V. Wenckstern, *Adv. Electron. Mater.* **2017**, *3*, 1600350.
[14] S. Sampath Kumar, E. J. Rubio, M. Noor-A-Alam, G. Martinez, S. Manandhar, V. Shutthanandan, *J. Phys. Chem.* **2013**, *117*, 4194.
[15] K. Ishibashi, R. Aida, M. Takahara, J. Kudo, I. Tsunoda, K. Takakura, T. Nakashima, M. Shibuya, K. Murakami, *Phys. Status Solidi C* **2013**, *10*, 1588.
[16] M. Passlack, E. F. Schubert, W. S. Hobson, M. Hong, N. Moriya, S. N. G. Chu, K. Konstadinidis, J. P. Mannaerts, M. L. Schnoes, G. J. Zydzik, *J. Appl. Phys.* **1995**, *77*, 686.
[17] P. Marie, X. Portier, J. Cardin, *Phys. Status Solidi A* **2008**, *205*, 1943.
[18] E. G. Villora, K. Shimamura, K. Kitamura, K. Aoki, *Appl. Phys. Lett.* **2006**, *88*, 031105.
[19] K. Sasaki, A. Kuramata, T. Masui, E. G. Villora, K. Shimamura, S. Yamakoshi, *Appl. Phys. Express* **2012**, *5*, 035502.
[20] M. Kracht, A. Karg, J. Schlörmann, M. Weinhold, D. Zink, F. Michel, M. Rohnke, M. Schowalter, B. Gerken, A. Rosenauer, P. J. Klar, J. Janek, M. Eickhoff, *Phys. Rev. Appl.* **2017**, *8*, 054002.
[21] N. M. Sbrockey, T. Salagaj, E. Coleman, G. S. Tompa, Y. Moon, M. S. Kim, *J. Electron. Mater.* **2015**, *44*, 1357.
[22] M. Orita, H. Hiramatsu, H. Ohta, M. Hirano, H. Hosono, *Thin Solid Films* **2002**, *411*, 134.
[23] Y. Li, A. Trinchi, W. Wlodarski, K. Galatsis, K. K. Zadeh, *Sens. Actuators B* **2003**, *93*, 431.
[24] Y. Kokubun, K. Miura, F. Endo, S. Nakagomi, *Appl. Phys. Lett.* **2007**, *90*, 031912.
[25] E. Auer, A. Lugstein, S. Loffler, Y. J. Hyun, W. Brezna, E. Bertagnolli, P. Pongratz, *Nanotechnology* **2009**, *20*, 434017.
[26] T. Terasako, H. Ichinotani, M. Yagi, *Phys. Status Solidi C* **2015**, *12*, 985.
[27] S. Rafique, L. Han, H. Zhao, *Phys. Status Solidi A* **2016**, *213*, 1002.
[28] L. Jianjun, Y. Jinliang, S. Liang, L. Ting, *J. Semicond.* **2010**, *31*, 103001.
[29] H. C. Kang, *Mater. Lett.* **2014**, *119*, 123.
[30] C. V. Ramana, E. J. Rubio, C. D. Barraza, A. Miranda Gallardo, S. McPeak, S. Kotru, J. T. Grant, *J. Appl. Phys.* **2014**, *115*, 043508.
[31] J. Castillo, R. Garcia-Perez, H. Huq, *J. Electron. Mater.* **2019**, *48*, 536.
[32] T. Oshima, T. Okuno, S. Fujita, *Jpn. J. Appl. Phys.* **2007**, *46*, 7217.
[33] F. B. Zhang, K. Saito, T. Tanaka, M. Nishio, Q. X. Guo, *J. Cryst. Growth* **2014**, *387*, 96.
[34] M. Rebien, W. Henrion, M. Hong, J. P. Mannaerts, M. Fleischer, *Appl. Phys. Lett.* **2002**, *81*, 250.
[35] I. Baía, M. Quintela, L. Mendes, P. Nunes, R. Martins, *Thin Solid Films* **1999**, *337*, 171.
[36] M. Ahmadipour, S. N. Ayub, M. F. Ain, Z. A. Ahmad, *Mater. Sci. Semicond. Process.* **2017**, *66*, 157.
[37] J. Tauc, R. Grigorovici, A. Vancu, *Phys. Status Solidi* **1966**, *15*, 627.
[38] H. Nalwa, *Deposition and Processing of Thin Films*, Academic Press, San Diego **2002**, p. 416.
[39] A. Bikowski, T. Welzel, K. Ellmer, *Appl. Phys. Lett.* **2013**, *102*, 242106.
[40] H. Salmang, H. Scholze, *Keramik* (Hrsg. R. Telle), Springer-Verlag Berlin, Heidelberg, New York **2007**.

© 2019 The Authors. physica status solidi (a) applications and materials science published by Wiley-VCH GmbH